frontiers in Ecology and Evolution

ORIGINAL RESEARCH
published: 07 April 2020
doi: 10.3389/fevo.2020.00069

Cranial Anatomy and Paleoneurology of the Extinct Sloth *Catonyx tarijensis* (Xenarthra, Mylodontidae) From the Late Pleistocene of Oruro, Southwestern Bolivia

Alberto Boscaini[1]*, *Dawid A. Iurino*[2,3], *Bernardino Mamani Quispe*[4], *Rubén Andrade Flores*[4], *Raffaele Sardella*[2,3], *François Pujos*[1] and *Timothy J. Gaudin*[5]

[1] Instituto Argentino de Nivología, Glaciología y Ciencias Ambientales (IANIGLA), CCT-CONICET-Mendoza, Mendoza, Argentina, [2] Dipartimento di Scienze della Terra, Sapienza Università di Roma, Rome, Italy, [3] Paleo Factory, Sapienza Università di Roma, Rome, Italy, [4] Departamento de Paleontología, Museo Nacional de Historia Natural de Bolivia, La Paz, Bolivia, [5] Department of Biology, Geology, and Environmental Sciences, University of Tennessee at Chattanooga, Chattanooga, TN, United States

OPEN ACCESS

Edited by:
Lorenzo Rook,
University of Florence, Italy

Reviewed by:
Marina Melchionna,
University of Naples Federico II, Italy
Luciano Varela,
Universidad de la República, Uruguay
Gerardo De Iuliis,
University of Toronto, Canada

***Correspondence:**
Alberto Boscaini
aboscaini@mendoza-conicet.gob.ar;
alberto.boscaini@gmail.com

Specialty section:
This article was submitted to Paleontology, a section of the journal Frontiers in Ecology and Evolution

Received: 25 December 2019
Accepted: 04 March 2020
Published: 07 April 2020

Citation:
Boscaini A, Iurino DA, Mamani Quispe B, Andrade Flores R, Sardella R, Pujos F and Gaudin TJ (2020) Cranial Anatomy and Paleoneurology of the Extinct Sloth Catonyx tarijensis (Xenarthra, Mylodontidae) From the Late Pleistocene of Oruro, Southwestern Bolivia. Front. Ecol. Evol. 8:69. doi: 10.3389/fevo.2020.00069

Extinct scelidotheriine sloths are among the most peculiar fossil mammals from South America. In recent decades, the external cranial anatomy of Pleistocene scelidotheres such as *Scelidotherium*, *Catonyx*, and *Valgipes* has been the subject of numerous studies, but their endocranial anatomy remains almost completely unknown. Today, computed tomographic (CT) scanning methodologies permit the exploration of previously inaccessible anatomical areas through a completely non-destructive process. For this reason, we undertook an analysis of the external and internal cranial anatomy of *Catonyx tarijensis* from the late Pleistocene of the Department of Oruro, in southwestern Bolivia. One particularly well-preserved specimen allowed detailed observation of all the main cranial osteological features, including the ear region and an almost complete hyoid apparatus, previously unknown for this taxon. Moreover, CT-scanning and subsequent elaboration of digital models of this specimen allowed observation of the brain cavity and cranial sinuses, and reconstruction of the trajectory of the main cranial nerves for the first time in an extinct scelidotheriine sloth. Additionally, we recovered the first three-dimensional reconstructions of the nasal cavity and the turbinates of an extinct sloth. In contrast to the usual depiction, the combined information from the external and internal anatomy suggests reduced lingual protrusion in *Catonyx tarijensis*, or at least a consistently more limited protrusion of the tongue in comparison with other mylodontid sloths such as *Glossotherium robustum*. The new morphological information recovered from this extinct sloth is compared with the available information for both extant and extinct forms, providing insights in the paleobiology of the extinct species. The present study reveals the importance of applying these novel non-destructive techniques to elucidate the evolutionary history of sloths.

Keywords: Xenarthra, scelidotheriine sloth, *Catonyx tarijensis*, skull, anatomy, endocast, hyoid apparatus

INTRODUCTION

Sloths (Folivora) are today represented by only two genera, *Bradypus* and *Choloepus,* and constitute an endemic South and Central American mammalian clade restricted to Neotropical rain forests (Nowak, 1999). By contrast, their fossil record is extremely rich and diverse, spanning chronologically from the late Eocene to the early Holocene, and geographically covering nearly all of the American supercontinent (e.g., McNab, 1985; Steadman et al., 2005; Gaudin and Croft, 2015). Mylodontidae is one of the most important folivoran clades, representing a major subdivision of sloths' diversity (e.g., Gaudin, 2004; Boscaini et al., 2019a; Delsuc et al., 2019; Presslee et al., 2019). Its representatives were mainly quadrupedal and terrestrial, and in some cases developed digging capabilities (e.g., Vizcaíno et al., 2001; Pujos et al., 2012). Mylodontid sloths were particularly widespread and abundant in South America, but they also reached Central and North America in different migratory events (e.g., Robertson, 1976; Webb, 1989; McDonald and Pelikan, 2006).

Among mylodontids, Mylodontinae includes medium to large-sized herbivorous forms and, with a few exceptions (e.g., *Mylodon* and *Pseudoprepotherium*; see Hirschfeld, 1985 and Bargo et al., 2006), they show mediolaterally wide muzzles that are indicative of grazing diets (McDonald, 1997; Bargo et al., 2006; Pujos et al., 2012). A different morphology is observed in the sister group to Mylodontinae, Scelidotheriinae. The narrow muzzle of scelidotheriines have been associated with more selective diets (McDonald, 1997; Bargo et al., 2006). Indeed, scelidotheriine sloths have long been recognized as distinctive, based on their unusual dentition and skull morphology (e.g., Owen, 1839; Gervais and Ameghino, 1880; McDonald, 1987). McDonald (1987) noted that all scelidotheriine species possess elongated and narrow skulls. The dentition is also buccolingually compressed, so that every tooth has a long axis that is much longer than its orthogonal width, although the orientation of the long axis varies along the toothrow (Owen, 1839; Gervais and Ameghino, 1880; McDonald, 1987). Gaudin (2004) identified additional unique synapomorphies of Scelidotheriinae. For example, the maxilla is deeper in its midsection to accommodate the elongated tooth roots, and narrows anteriorly and posteriorly, in lateral view (Gaudin, 2004). This results in a ventrally convex profile of the palate in lateral view that is also unique to the group (Gaudin, 2004).

The scelidotheriine fossil record ranges chronologically from the middle Miocene to the Pleistocene/Holocene transition (Friasian to Bonaerian/Lujanian SALMAs; South American Land Mammal Age(s); McDonald, 1997; Scillato-Yané and Carlini, 1998; McDonald and De Iuliis, 2008; Miño-Boilini et al., 2019). In contrast to mylodontines, scelidotheriines were restricted to South America, and did not participate in the G.A.B.I. (Great American Biotic Interchange), as a probable consequence of their ecological restrictions due to specialized feeding habits (McDonald, 2005; Amson et al., 2016). During the Pleistocene, this clade was represented by three genera: (i) *Valgipes*, endemic to the intertropical region of Brazil (Cartelle et al., 2009, 2019), (ii) *Scelidotherium*, from the Pampas region of Argentina and Uruguay (McDonald and De Iuliis, 2008; Corona et al., 2013), and (iii) *Catonyx* (=*Scelidodon*) a more widespread taxon known from Argentina, Bolivia, Brazil, Chile, Ecuador, Peru, and Uruguay (Miño-Boilini, 2016).

According to Gaudin (2004), features that serve to differentiate the two scelidotheriine *Catonyx* and *Scelidotherium* include: the posterior extension of the temporal fossa, which is more pronounced in the former taxon (Gaudin, 2004: char. 97); in *Catonyx*, the orbital portion of the lacrimal is more expanded than the facial, whereas the two portions are equal in size in *Scelidotherium* (Gaudin, 2004: char. 140); a maxillo-lacrimal contact within the orbit is present in *Catonyx*, whereas it is absent in *Scelidotherium* (Gaudin, 2004: char. 109); the sphenorbital fissure is more posteriorly located in *Scelidotherium* than in *Catonyx* (Gaudin, 2004: char. 161), and *Scelidotherium* exhibits a smaller hypoglossal foramen than *Catonyx* (Gaudin, 2004: char. 187). Finally, *Catonyx* possesses distinct fossae for the rectus capitis muscles on the basioccipital that are lacking in *Scelidotherium* (Gaudin, 2004: char. 196).

Following the latest revisions of the group (i.e., McDonald and Perea, 2002; Corona et al., 2013; Miño-Boilini, 2016), *Catonyx* includes three species: (i) *C. chiliensis* from the Lujanian SALMA of Argentina, Bolivia, Chile, Ecuador, and Peru, (ii) *C. cuvieri* from the Lujanian SALMA of Brazil and Uruguay, and (iii) *C. tarijensis*, from the Ensenadan–Lujanian SALMAs of Argentina, Bolivia, and Uruguay. Only *C. chiliensis* and *C. tarijensis* have previously been recovered from Bolivia. The two species are easily recognizable by their general body size, the shape of the nasals, the development of the sagittal crest, and the morphology of the dentition in occlusal view (McDonald, 1987; McDonald and Perea, 2002; Corona et al., 2013; Miño-Boilini, 2016).

In the present contribution, based on an almost complete skull of *Catonyx tarijensis* from late Pleistocene deposits of the Department of Oruro, we provide a detailed description of its skull and mandible, with special emphasis on its poorly known ear region. We also provide a description of the almost complete hyoid apparatus of this species, together with the first digital reconstructions of the main endocranial structures of a scelidotherine sloth.

MATERIALS AND METHODS

The specimen of *Catonyx tarijensis* MNHN-Bol V 13364 analyzed in the present study was recovered in 2013 from late Pleistocene deposits at Chokxo Pata, Ayllu Yuruma locality (18° 43′ 28.5″ S; 67° 26′ 39.8″ W; altitude: 3.667 m a.s.l.). This locality is situated on the western side of Lake Poopó (Municipality of Santiago de Andamarca, Sud Carangas Province, Department of Oruro, southwestern Bolivia; **Figure 1**). The specimen was recovered in a friable non-laminated yellowish sandstone of lacustrine origin, without any other associated faunistic elements. However, the late Pleistocene age of the fossils is suggested by the unconsolidated nature of the sediments and low degree of

Abbreviations: MNHN, Muséum national d'Histoire naturelle, Paris, France; MNHN-Bol, Museo Nacional de Historia Natural de Bolivia, La Paz, Bolivia.

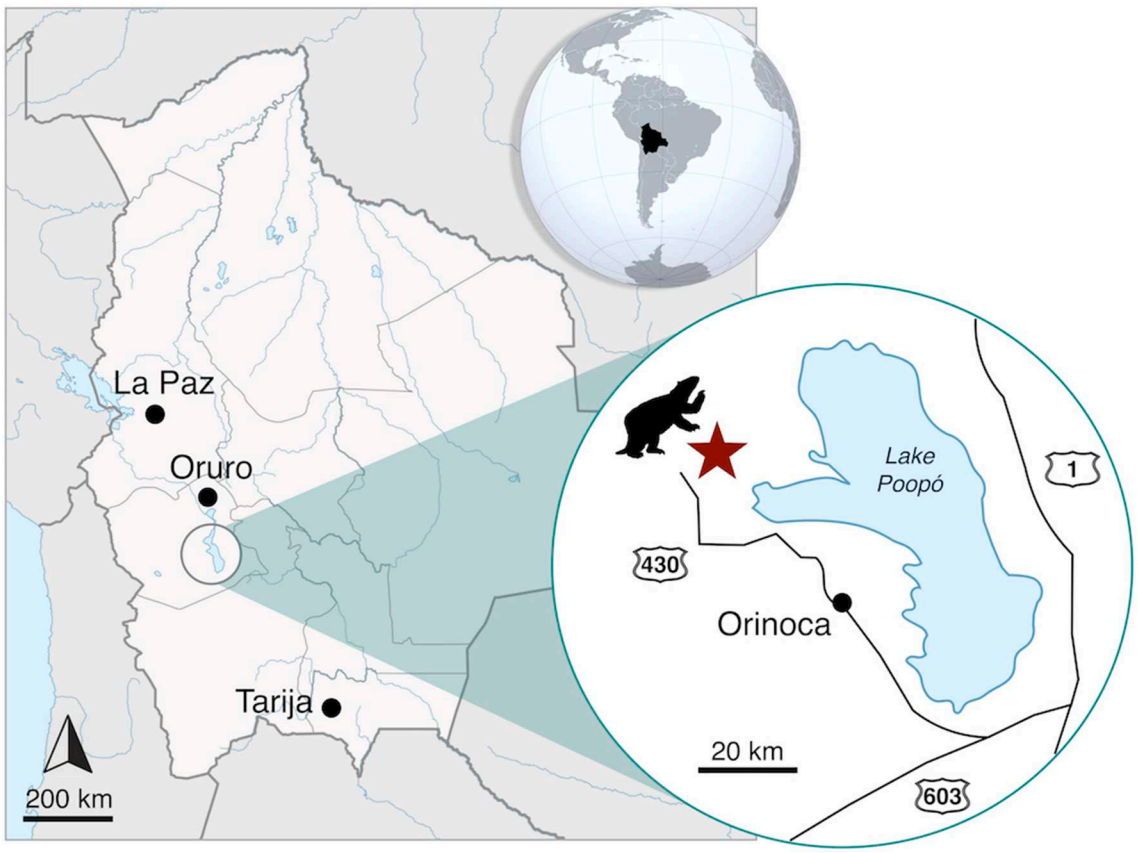

FIGURE 1 | Map of the locality in which the remains of *Catonyx tarijensis* MNHN-Bol V 13364 have been recovered. Circles: cities; Star: fossil locality.

petrification of the remains, together with absolute dates obtained in neighboring areas (Placzek et al., 2006). At the moment, a late Pleistocene age for these remains is the most plausible, given the wide distribution of *Catonyx* in other South American localities in this period (see Introduction). However, further paleontological surveys and detailed analyses at Chokxo Pata are necessary for a reliable chronological assessment of the recovered remains. The specimen labeled as MNHN-Bol V 13364 includes an almost complete skull, both mandibular rami, most of the hyoid apparatus, an incomplete left humerus and radius, and other postcranial fragments.

MNHN-Bol V 13364 is particularly well-preserved and exhibits only slight deformation, allowing detailed descriptions of the cranial and mandibular remains, with special emphasis on the ear region and the hyoid apparatus. Moreover, we report the first digital models of the endocranial cavities of a scelidotheriine sloth, based on scans of MNHN-Bol V 13364, taken with a Somatom Scope (Siemens) CT scanner at the "Clínica Alemana" Institute of La Paz (Bolivia). The scanning resulted in 1,032 slices with a slice thickness of 0.75 mm. The image segmentation process was performed using the digital tools provided by OsiriX v.5.6 32-bit and Materialize Mimics v.20. The 3D models of the nasal cavity, turbinates, brain cavity, and cranial sinuses were exported from Mimics as ".PLY" files, then converted to ".OBJ" format and imported into ZBrush 4R6 for the rendering process. Unfortunately, the resolution of the CT-scan did not allow for a detailed reconstruction of the bony labyrinth of MNHN-Bol V 13364, and for this reason this anatomical area is not treated in the present paper.

External craniodental measurements were taken with a digital caliper to the nearest 0.1 mm, whereas measurements of the digital models were obtained using the tools of the software Materialize Mimics v.20.

The comparative sample is largely based on the dataset assembled by Boscaini et al. (2020), which includes the two extant sloth species *Bradypus variegatus* and *Choloepus hoffmanni*, and the extinct giant mylodontine *Glossotherium robustum*. For the purposes of comparison, other non-digital endocranial information was obtained from Gervais (1869) and Dechaseaux (1958, 1962a,b, 1971).

RESULTS

Systematic Paleontology

XENARTHRA (Cope, 1889)
PILOSA (Flower, 1883)
FOLIVORA (Delsuc et al., 2001)
MYLODONTIDAE (Gill, 1872)

SCELIDOTHERIINAE (Ameghino, 1904)
Catonyx (Ameghino, 1891)
Catonyx tarijensis (Gervais and Ameghino, 1880)

Holotype MNHN.F.TAR1260, skull and mandible from the Pleistocene of Tarija Valley (southern Bolivia).

Referred material MNHN-Bol V 13364: complete skull, associated with both mandibular rami and most of the hyoid apparatus, incomplete left humerus and radius, and isolated postcranial fragments from late Pleistocene deposits at Chokxo Pata, Ayllu Yuruma locality (Sud Carangas Province, Department of Oruro, southwestern Bolivia).

Measurements see **Table 1**.

Type locality and age Department of Tarija (southern Bolivia), Tolomosa Formation, middle (0.76 ± 0.03 Ma; U–Th/Pb and U–Th/H; MacFadden et al., 2013) or late (44-21 ka; C^{14}; Coltorti et al., 2007) Pleistocene.

Distribution Pleistocene deposits of Bolivia, Argentina and Uruguay (McDonald and Perea, 2002; Corona et al., 2013; Miño-Boilini, 2016).

Comparative Description of the External Anatomy

Skull

The skull of *Catonyx tarijensis* MNHN-Bol V 13364 is tubular in section, anteroposteriorly elongated, and somewhat low dorsoventrally (**Figure 2**), all typical of scelidotheriine cranial morphology (e.g., McDonald, 1987; Gaudin, 2004; Miño-Boilini, 2012).

The medial and lateral anterior processes of the nasal are separated by a deep notch (**Figures 2A,C**), as is typical in scelidotheriines (Gaudin, 2004: char. 102). The anterior portion of the nasal is mediolaterally expanded and tapers posteriorly in a gradual and uniform fashion. The nasofrontal suture is almost transverse and straight (**Figure 2A**).

Only the posteriormost portion of the right premaxilla is present, preserving a minor portion of the lateral ramus (**Figure 2B**). The palatal portion of the maxilla exhibits a ventrally convex profile in lateral view (**Figure 2C**), a characteristic feature of scelidotheriines (Gaudin, 2004: char. 121; Cartelle et al., 2009). The palate itself is elongated and narrow, and extends well posterior to the last upper molariform as a broad postpalatal shelf that extends posteriorly along the medial surface of the pterygoid flange for almost half its anteroposterior length (**Figure 2B**). This shelf is pierced by at least one large postpalatal foramen (=minor palatine foramen of other mammals; Gaudin, 2011). The anterior palatal foramen is only preserved on the right side, where it forms a small opening emptying into a short, shallow anterior groove, roughly halfway between the lateral ramus of the premaxilla and the first molariform. The incisive foramina are largely hidden by the large medial palatal processes of the maxilla (as in *Scelidotherium*; Gaudin, 2004: char. 117) and are located within an elongate median groove at the anterior end of the palate (**Figure 2B**). The anterior end of the maxillopalatine suture lies medial to the third molariform, as it does in *Scelidotherium* (Gaudin, 2004: Figure 5B).

TABLE 1 | External and internal measurements of the craniodental remains of *Catonyx tarijensis* MNHN-Bol V 13364 from the Pleistocene of Oruro (Bolivian Altiplano).

Measurement	Value
Skull	
Basicranial width	200.8
Condyle external width	142.1
Condyle internal width	69.4
Foramen magnum height	49.7
Maxillary extension (anterior to Mf1)	91.8
Maxillo-condylar length	501.1
Maximum snout width	120
Minimum post-orbital width of the frontal	121.1
Minimum snout width	115.3
Occipital height	128.4
Palatal length (excluding the premaxilla)	232.7
Palatal width (at the level of Mf2)	58.4
Palatal width (at the level of Mf5)	48.8
Snout height	123.6
Snout length	104.6
Upper dental series length	120.8
Mandible	
Condyle-angle height	121.4
Coronoid process anteroposterior length	86.5
Height of ramus at the level of mf1	86.2
Height of ramus at the level of mf2	91.6
Height of ramus at the level of mf3	91.7
Height of ramus at the level of mf4	92.8
Lower dental series length	111.2
Mandibular condyle length	23.3
Mandibular condyle width	50.7
Symphyseal spout length	113.3
Symphyseal spout width	68.7
Total length of mandible	411.4
Upper dentition	
Mf1 mesiodistal length	23.6
Mf1 buccolingual width	11.2
Mf2 mesiodistal length	24.6
Mf2 buccolingual width	15.4
Mf3 mesiodistal length	24.1
Mf3 buccolingual width	15.3
Mf4 mesiodistal length	20.1
Mf4 buccolingual width	13.8
Mf5 mesiodistal length	13.9
Mf5 buccolingual width	13.4
Lower dentition	
mf1 mesiodistal length	29.7
mf1 buccolingual width	16.8
mf2 mesiodistal length	26.2
mf2 buccolingual width	10.6
mf3 mesiodistal length	26.1
mf3 buccolingual width	11.5
mf4 mesiodistal length	36.2
mf4 buccolingual width	20.9
Brain endocast	
Maximum anteroposterior length	155.6
Maximum mediolateral width	100.2
Volume (including nerves)	571.9

Mf, upper molariform tooth; mf, lower molariform tooth. Measurements are reported in mm, except for the brain endocast volume which is reported in cm^3.

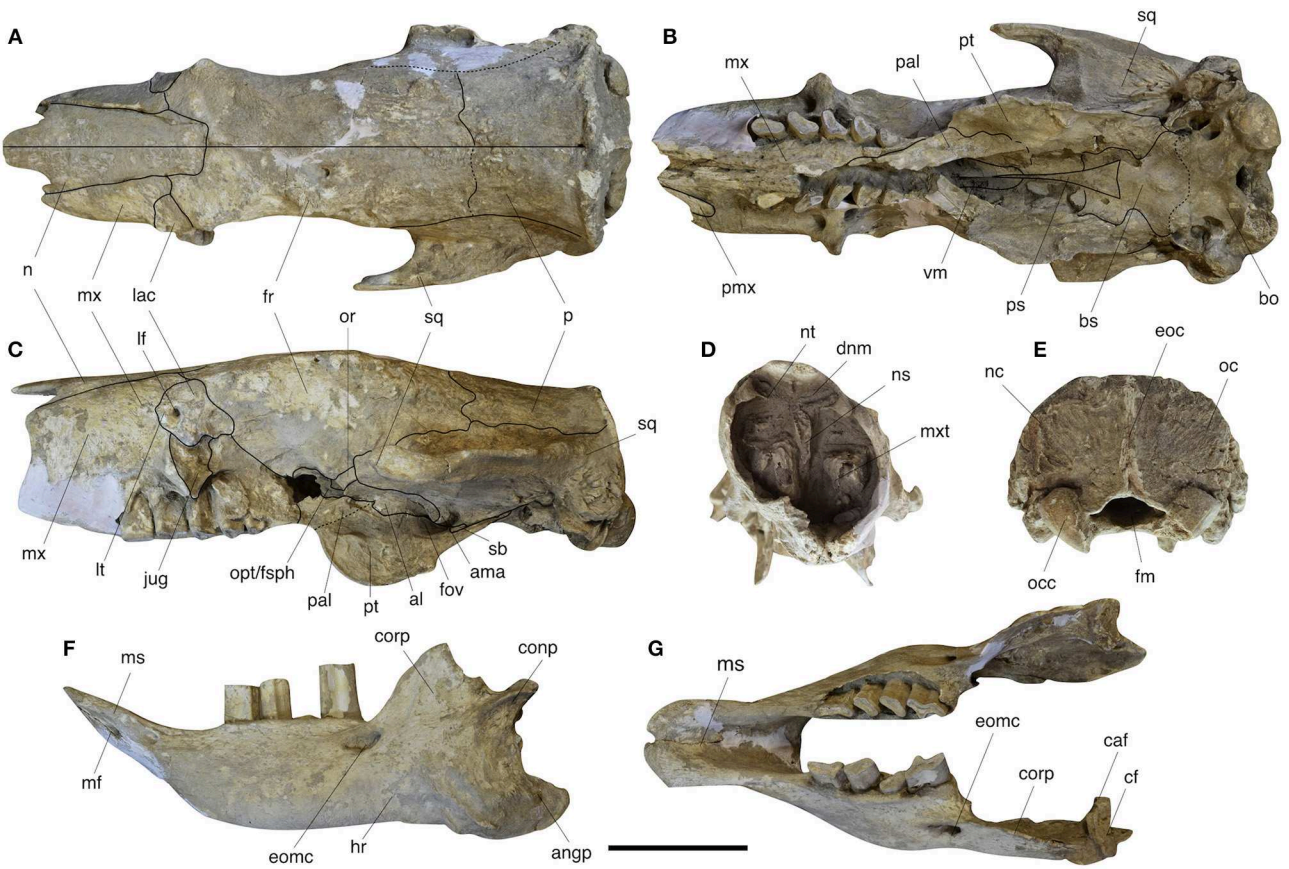

FIGURE 2 | Skull and mandible of *Catonyx tarijensis* MNHN-Bol V 13364 from the Pleistocene of Oruro (Bolivian Altiplano). Skull in dorsal **(A)**, ventral **(B)**, lateral **(C)**, anterior **(D)**, and posterior **(E)** views. Mandible in lateral **(F)** and occlusal **(G)** views. al, alisphenoid; ama, accessory mandibular articulation; angp, angular process; bo, basioccipital; bs, basisphenoid; caf, condylar accessory facet; cf, condylar facet; conp, condyloid process; corp, coronoid process; dnm, dorsal nasal meatus; eoc, external occipital crest; eomc, external opening of the mandibular canal; fm, foramen magnum; fov, foramen ovale; fr, frontal; hr, horizontal ramus of mandible; jug, jugal; lac, lacrimal; lf, lacrimal foramen; lt, lacrimal tubercle; mf, mental foramen; ms, mandibular spout; mx, maxilla; mxt, maxilloturbinate; n, nasal; nc, nuchal crest, ns, nasal septum; nt, nasoturbinate; oc, occipital; occ, occipital condyle; opt/fsph, common aperture for the optic foramen and sphenorbital fissure; or, orbitosphenoid; pal, palatine; p, parietal; pmx, premaxilla; ps, presphenoid; pt, pterygoid; sb, sutural bone; sq, squamosal; vm, vomer. Scale bar equals 10 cm.

The lacrimal is roughly quadrilateral in shape and has a relatively reduced facial exposure and an extensive orbital exposure (**Figure 2C**). In this respect, *Catonyx* differs from *Scelidotherium*, in which the orbital exposure is no larger than the facial (Gaudin, 2004: char. 140). There is a well-developed lacrimal tubercle just anterior to the single large and circular lacrimal foramen (**Figure 2C**). The latter is located on the facial portion of the lacrimal and just anterior to the orbital rim. The facial exposure of the lacrimal contacts the maxilla anteriorly and the frontal posteriorly. This contrasts with the information in Gaudin (2004: char. 107), in which a contact between the nasal and lacrimal is considered a synapomorphy of scelidotheres, suggesting that this feature may represent a variable feature at different taxonomic levels. The absence of contact between the nasal and the lacrimal in MNHN-Bol V 13364, differs from the arrangement depicted by McDonald (1987) for the same species. The variability of this feature was first mentioned by Kraglievich (1923) for *Scelidotherium* and is now also confirmed for *Catonyx*. In MNHN-Bol V 13364, the orbital exposure of the lacrimal contacts the jugal and the maxilla ventrally and the frontal posteriorly (**Figure 2C**). The contact between maxilla and lacrimal within the orbit is absent in *Scelidotherium* (Gaudin, 2004: char. 109).

Another distinctive feature of MNHN-Bol V 13364 is the exceptional preservation of the nasopharyngeal roof (**Figure 2B**). At the anterior end, both the alae and the median keel of the vomer are visible, the former well-outlined by sutures (**Figure 2B**). A typical triangular presphenoid is observable posterior to the vomer. The basisphenoid is irregular in shape but reminiscent of the butterfly shape commonly observed in some mylodontids, such as *Mylodon*, *Glossotherium*, and *Paramylodon* (Patterson et al., 1992) and other sloths, such as *Bradypus* and *Analcimorphus* (Gaudin, 2004: char. 198). The basisphenoid and basioccipital are completely fused. However, there are two strongly developed tubera which typically lie on the junction between the basisphenoid and the basioccipital, suggesting that

the suture occurs in this region (**Figure 2B**). The basioccipital is wide transversely and short anteroposteriorly, nearly flat but marked bilaterally by shallow depressions for the rectus capitis muscles (**Figure 2B**). As noted above, these fossae are absent in *Scelidotherium*.

As is common in mylodontids, there is a large ovate depression near the bottom of the medial orbital wall that houses most of the major orbital foramina (**Figure 2C**). The sphenopalatine/anterior palatal foramen, which is normally part of this complex, is not preserved on either side. However, the large opening, typical of sloths (Gaudin, 2004: char 160), that serves as a common aperture for the optic foramen and sphenorbital fissure, is well-preserved bilaterally (**Figure 2C**). *Scelidotherium* differs from *Catonyx* in the absence of a common depression for the orbital foramina, with the aperture of the optic foramen/sphenorbital fissure situated well posterior to the sphenopalatine/anterior palatal foramen (Gaudin, 2004: char. 161). The sutural relationships of the bones surrounding the aperture for the optic foramen/sphenorbital fissure are complex in MNHN-Bol V 13364 (**Figure 2C**). Indeed, four bones participate in the formation of the opening: frontal, orbitosphenoid, alisphenoid, and palatine. The frontal forms the anterior and dorsalmost portion of the aperture. The orbitosphenoid forms the roof and part of the lateral wall. The alisphenoid is the most complex, comprising a portion of the lateral wall, most of the medial wall, as well as a portion of the floor. The remaining part of the floor of the aperture is formed by the palatine (**Figure 2C**). The orbitosphenoid has a small lateral exposure lateral to the aperture of the sphenorbital fissure/optic foramen, extending posteriorly to contact the squamosal and largely separating the alisphenoid and frontal. A lateral exposure of the orbitosphenoid like this is quite unusual, not only in sloths, but for xenarthrans in general, but has been reported in a single juvenile specimen of the extant two-toed sloth *Choloepus hoffmanni* (Gaudin, 2011).

The foramen ovale of MNHN-Bol V 13364 is located between the alisphenoid, pterygoid, and squamosal. The last two elements form the bulk of the rim, with the alisphenoid contributing only a small portion of the anterior edge. In MNHN-Bol V 13364 there is also a rounded projection extending ventrally from the dorsolateral margin of the foramen ovale and partially shielding it in lateral view (**Figure 2C**). This small projection is comprised of alisphenoid anteriorly and squamosal posteriorly, and bears a slightly concave articular surface laterally (**Figure 2C**). This surface contacts a distinct medial facet on the mandibular condyle, and therefore we identify this as an accessory mandibular articulation (ama; **Figure 2C**), unknown in other sloths.

Behind the foramen ovale, an ovoid, reduced sutural bone is present, just at the junction between the pterygoid and the squamosal (**Figure 2C**). The pterygoid/squamosal suture extends posteriorly into the ear region (**Figures 2B,C**). The pterygoid of *C. tarijensis* appears less inflated basally than is the case in either *M. darwinii* or *G. robustum* (Patterson et al., 1992; Boscaini et al., 2018a). In the latter two taxa, a pair of inflated areas, lateral and medial, are observed at the base of the pterygoid, whereas in *C. tarijensis*, a single low pterygoid inflation is present (**Figure 2B**). The ventral portion of the pterygoid extends ventrally into a large pterygoid flange, as is typical for sloths (Gaudin, 2004). In *Catonyx,* the ventral margin of this flange is semicircular in shape, whereas in *Scelidotherium* it is more nearly triangular (Owen, 1857; Gaudin, 2004: Figure 5A).

In MNHN-Bol V 13364 many of the internal structures of the nasal cavity are visible in anterior view, including the nasal septum and the anteriormost portion of the nasoturbinates and maxilloturbinates (**Figure 2D**). The nasoturbinates terminate anteriorly on the underside of the long lateral process of the nasal and delimit the dorsal nasal meatus ventrally. The surface of the maxilloturbinates form a relatively smooth and conical mass at its anterior end (**Figure 2D**).

In dorsal view, the temporal lines are poorly developed and the sagittal crest is lacking (**Figure 2A**), two features that are probably related to the immaturity of the individual (Corona et al., 2013). In MNHN-Bol V 13364, the temporal lines are only observable at the level of the poorly developed postorbital processes, and posteriorly, where they merge with the nuchal crest (**Figure 2A**). Among Mylodontidae, the posterior convergence of the temporal lines and the nuchal crest is also observed in *Nematherium*, *Octodontotherium*, and Lestodontini (Gaudin, 2004: char. 97). In *Scelidotherium* and other mylodontines, the temporal lines turn ventrally, anterior to the nuchal crest. The frontoparietal suture is only partially detectable in MNHN-Bol V 13364 (**Figure 2A**), and shows an irregular and bilaterally asymmetric outline. The position of this suture, well posterior to the glenoid, represents a scelidotheriine + mylodontine synapomorphy according to Gaudin (2004: char. 172).

In posterior view (**Figure 2E**), the occipital is subrectangular in shape, as is typical for scelidotheriines (Brambilla and Ibarra, 2018), whereas the subtriangular occipital condyles are directed ventrally, as is typical for *Catonyx* (Corona et al., 2013; Miño-Boilini, 2016).

Ear Region

The ectotympanic and the middle ear ossicles are missing on both sides of MNHN-Bol V 13364, but the remainder of the auditory region is well-preserved.

Both entotympanics are present and complete. As is typical for sloths, they are located lateral to the basioccipital/basisphenoid tuber and ventral to the promontorium of the petrosal (**Figures 2B**, **3**). Again as in most sloths, the entotympanic is divided into medial and lateral plates by a deep sulcus for the internal carotid artery (**Figure 3**; Gaudin, 1995). At the anterior end of this sulcus, the entotympanic encloses a canal through which the artery passed (**Figure 3**); the presence of this canal is a variable feature in *Catonyx* and *Scelidotherium* (Gaudin, 1995). A carotid foramen/canal in the entotympanic is also present in *Nematherium* and *Pseudoprepotherium*, but is missing in other mylodontids (Patterson et al., 1992; Gaudin, 1995, 2004).

On the right side of MNHN-Bol V 13364, the lateral plate of the entotympanic has a small opening near its anterior end that likely accommodated the exit of the greater petrosal nerve (=vidian nerve) from the tympanic cavity. A short groove for the greater petrosal nerve extends from the opening toward the

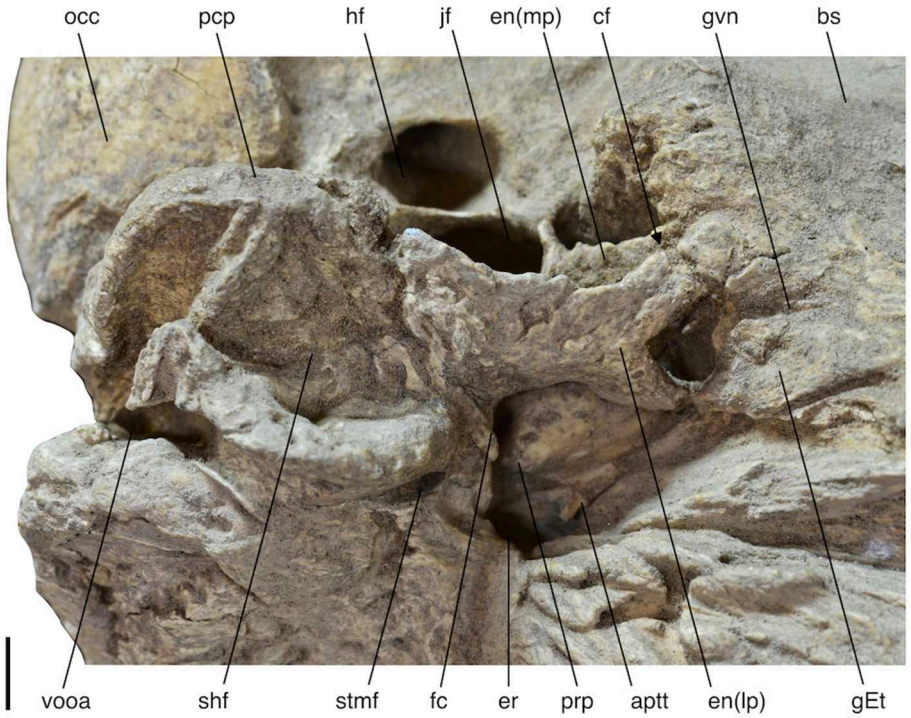

FIGURE 3 | Left ear region of *Catonyx tarijensis* MNHN-Bol V 13364 in ventrolateral view (anterior toward the right). aptt, anteroventral process of the tegmen tympani; bs, basisphenoid; cf, carotid foramen; en(lp), entotympanic (lateral plate); en(mp), entotympanic (medial plate); er, epitympanic recess; fc, fenestra cochleae; gEt, groove for the Eustachian tube; gvn, groove for the vidian nerve; hf, hypoglossal foramen; jf, jugular foramen; occ, occipital condyle; pcp, paracondylar process of exoccipital; prp, promontorium of petrosal; shf, stylohyal fossa; stmf, stylomastoid foramen; vooa, ventral opening for the occipital artery. Scale bar equals 1 cm.

nasopharynx. On the left side, there is a much larger aperture in roughly the same position (**Figure 3**), suggesting that this difference in size could be related to the immature development of this individual.

In fact, there are several additional features in the ear region which indicate the subadult status of MNHN-Bol V 13364 including: (i) a small gap between the medial entotympanic and the basioccipital/basisphenoid tuber (visible on the left side of the skull), (ii) an unusually deep stylohyal fossa, and (iii) the presence of an open groove for the occipital artery on the mastoid exposure of the petrosal (**Figure 3**). In all other mylodontids except *Nematherium*, the occipital artery is either partially or fully enclosed in a canal (Gaudin, 1995, 2004).

The petrosal morphology of MNHN-Bol V 13364 is typical for scelidotheres, and indeed for Mylodontidae as a whole (Patterson et al., 1992; Gaudin, 1995, 2004). One unusual aspect of this specimen is the small size of the anteroventral process of the tegmen tympani (aptt; **Figure 3**). The aptt is variable in size and shape among mylodontids, but was recorded as a "large, rugose bony mass" in prior observations of *Catonyx* (Gaudin, 1995, 2004). The small and triangular shape of the aptt in MNHN-Bol V 13364 (**Figure 3**) could also be related to its subadult status.

The large jugular foramen which marks the posteromedial boundary of the ear region is typical for mylodontids (**Figure 3**). However, the hypoglossal foramen is distinctive in a number of aspects. First, in MNHN-Bol V 13364 it is nearly identical in size to the jugular foramen (**Figure 3**), whereas in *Mylodon* and *Glossotherium* the hypoglossal foramen is larger than the jugular (Patterson et al., 1992; Boscaini et al., 2018a). Moreover, it nearly abuts the jugular foramen, the two being separated by a sharp ventral crest (**Figure 3**). In other mylodontids, the hypoglossal foramen is located farther posteriorly (Patterson et al., 1992; Boscaini et al., 2018a).

Mandible

The mandible of MNHN-Bol V 13364 shows an almost horizontal ventral border, as is typical for mylodontids (Gaudin, 2004; McDonald and De Iuliis, 2008). As in other scelidotheres, it has a very elongated and narrow mandibular spout with a rounded anterior edge (**Figures 2F,G**).

The very deep horizontal ramus of MNHN-Bol V 13364 (**Figure 2F**) is characteristic of *Catonyx tarijensis* and contrasts with the shallower ramus in *C. cuvieri* and *C. chiliensis* (Pujos, 2000; Miño-Boilini, 2016). The condyle is transversely extended as in other scelidotheres, but with a peculiar concave articular surface, which differs from the flat articular surface that is typical of the group (Gaudin, 2004: char. 55). The latter is bordered medially by a second articular surface for the accessory mandibular articulation, as discussed above.

Despite the apparent subadult status of the specimen, the grooves and ridges that mark the attachments of the masticatory muscles are very well-developed (**Figure 2F**). This is particularly

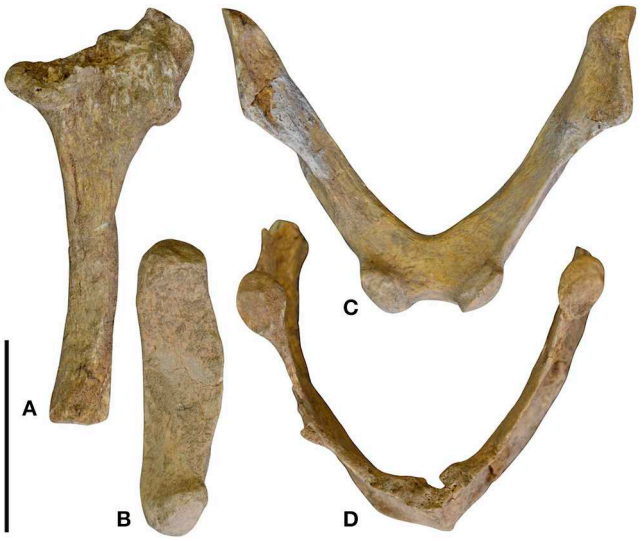

FIGURE 4 | Hyoid apparatus of *Catonyx tarijensis* MNHN-Bol V 13364 from the Pleistocene of Oruro (Bolivian Altiplano). Right stylohyal in medial view **(A)**; right epihyal in medial view **(B)**; V-bone in anterior view **(C)**; and ossified thyroid cartilage in anterior view **(D)**. Scale bar equals 5 cm.

evident along the ventrolateral margin of the angular process, where two strong grooves are present.

Hyoid Apparatus

A large part of the hyoid apparatus of MNHN-Bol V 13364 is preserved, the available elements including the right stylohyal and epihyal, the "V-bone" (fused basihyal and thyrohyals), and the ossified thyroid cartilage (**Figure 4**). Both ceratohyals, however, are missing. On the whole, the hyoid morphology of *Catonyx* reflects the general xenarthran pattern, which consists of three paired and unfused bones (representing the anterior cornua) and an unpaired V-bone (representing the posterior cornua) (Casali and Perini, 2017).

Stylohyal- The right stylohyal of MNHN-Bol V 13364 is almost complete, lacking only the articular facet for the basicranium (**Figure 4A**). The body of the stylohyal is cylindrical, with a slight enlargement toward the distal facet for the epihyal (**Figure 4A**), as is typical in Folivora (Gaudin, 2004: char. 79; Casali and Perini, 2017: char. 1). The shaft of the stylohyal is straight in *Catonyx* (**Figure 4A**), a condition that is observed in other scelidotheriines such as *Scelidotherium* and *Valgipes*, whereas the stylohyal shaft is curved in mylodontines such as *Mylodon*, *Paramylodon*, *Glossotherium*, and *Lestodon* (Gaudin, 2004; Pérez et al., 2010; Tambusso et al., 2015; Casali and Perini, 2017). However, the curved condition can be occasionally observed in some specimens of *Scelidotherium,* and the straight condition in some *Paramylodon* specimens (Casali and Perini, 2017). In *Paramylodon harlani*, Stock (1925) also identified an uncommon case of fusion between the stylohyal and the epihyal. This feature, commonly recovered among the extant sloths (Naples, 1986), is rarely observed in extinct taxa such as *Paramylodon harlani*, *Megatherium americanum*, and *Eremotherium laurillardi* (Casali and Perini, 2017). The stylohyal-epihyal contact is flat in lateral and medial views in MNHN-Bol V 13364 (**Figures 4A,B**). This feature is also typical of sclelidotheriines, in contrast to the more concavo-convex articulation of mylodontines (Pérez et al., 2010).

Epihyal- The epihyal of *Catonyx* MNHN-Bol V 13364 is shorter in length than the stylohyal (**Figures 4A,B**), a typical condition for pilosans (Gaudin, 2004: char 77; Casali and Perini, 2017: char. 2). The shaft of the epihyal is wide anteroposteriorly and compressed mediolaterally (**Figure 4B**), resembling the shape of the epihyal of *Scelidotherium* and in contrast to that observed in *Glossotherium* and *Paramylodon*, in which the epihyal decreases uniformly in width from its proximal to its distal end (Stock, 1925; Pérez et al., 2010). Both the facets for the stylohyal and the ceratohyal are flat (**Figure 4B**), again resembling the condition in *Scelidotherium* and contrasting with the morphology of *Paramylodon* and *Glossotherium*, in which they are concave and convex, respectively. Both ceratohyals are missing in MNHN-Bol V 13364. As in all extinct sloths, and in contrast to the living forms, they were unfused to the epihyals (Casali and Perini, 2017: char. 6).

V-bone and ossified thyroid cartilage- The fusion between the basihyal and the thyrohyals, forming the so-called V-bone, is a typical xenarthran feature (Pérez et al., 2010; Casali and Perini, 2017). The two anterior eminences that articulate with the ceratohyals are well-developed in *Catonyx* (**Figure 4C**) and similar in shape to those of *Glossotherium* and *Paramylodon* (Stock, 1925; Pérez et al., 2010). Posteriorly, the V-bone contacts the ossified thyroid cartilage through two roughly circular and flat facets (**Figure 4D**). In *Catonyx*, the V-bone and ossified thyroid cartilage are markedly V-shaped in anterior view (**Figures 4C,D**), similar to the morphology observed in *Scelidotherium* and distinct from the U-shaped homologous elements in *Glossotherium* and *Paramylodon* (Pérez et al., 2010).

Comparative Description of the Internal Anatomy

Nasal Cavity

The facial part of the respiratory tract is preserved, both externally (**Figure 2**) and internally (**Figure 5**). The main turbinates of this region, the nasoturbinate (an olfactory structure) and the maxilloturbinate (a respiratory structure), are observable in the anterior view of the nasal cavity (**Figure 2D**) and their morphology can be traced back posteriorly thanks to the digital endocranial reconstruction (**Figures 5A–D**).

The nasoturbinate of *Catonyx tarijensis* MNHN-Bol V 13364 is anteroposteriorly elongated and mediolaterally narrow. It is also inclined ventromedially in anterior view, facing the nasal septum. It constitutes the floor of the relatively large and undivided dorsal nasal meatus (**Figures 5A–D**). The nasoturbinate reaches the anterior edge of the nasal bone anteriorly (as noted above), and extends posteriorly to the level of the postorbital process of the frontal. Unfortunately, the ethmoidal crest and the ethmoturbinates are not preserved, preventing observation of the posterior attachment point for the nasoturbinates (**Figures 5A–C**). The nasoturbinates appear

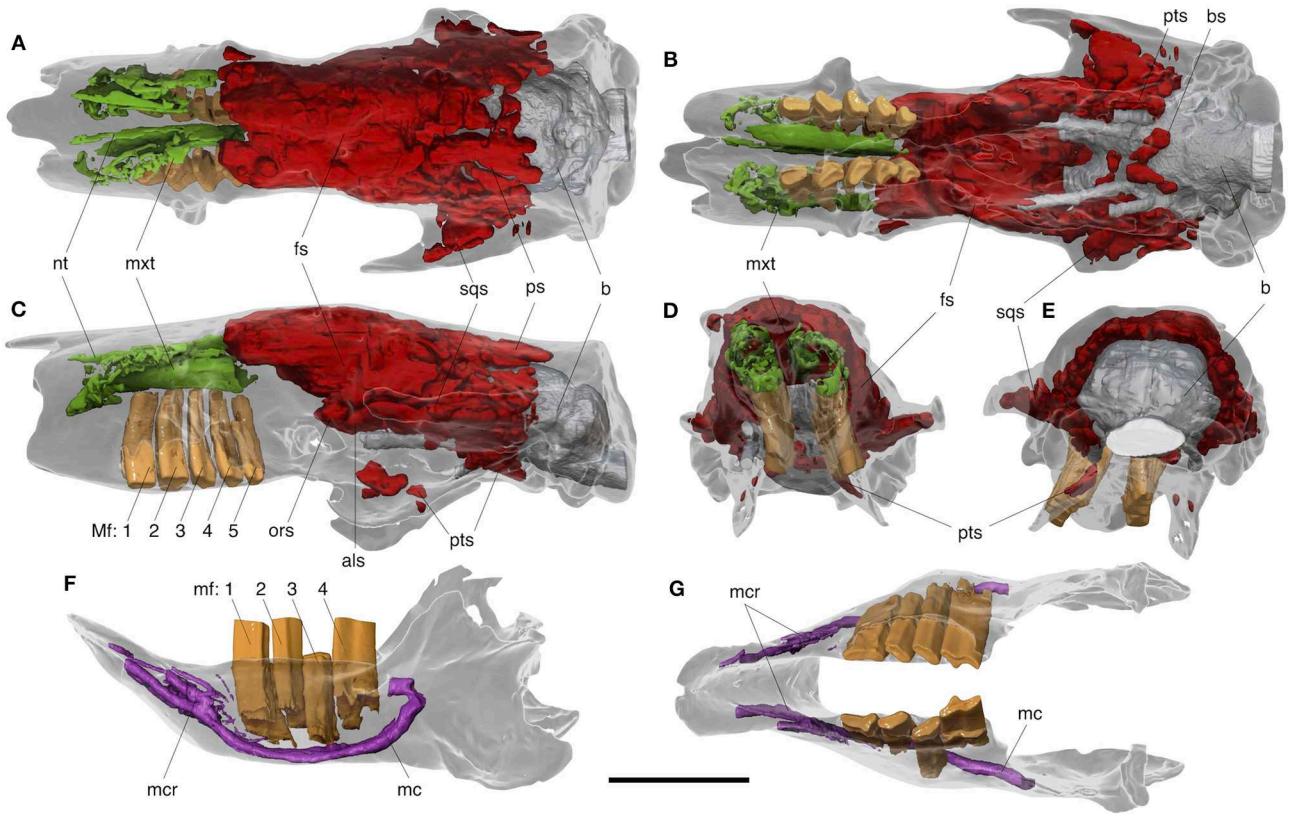

FIGURE 5 | Digital reconstructions of the skull and mandible of *Catonyx tarijensis* MNHN-Bol V 13364 from the Pleistocene of Oruro (Bolivian Altiplano), showing internal features. Skull in dorsal **(A)**, ventral **(B)**, lateral **(C)**, anterior **(D)**, and posterior **(E)** views. Mandible in lateral **(F)** and occlusal **(G)** views. als, alisphenoid sinus; b, brain endocast; fs, frontal sinus; mc, mandibular canal; mcr, mandibular canal ramifications; mf, lower molariform tooth; Mf, upper molariform tooth; mxt, maxilloturbinate; nt, nasoturbinate; ors, orbitosphenoid sinus; ps, parietal sinus; pts, pterygoid sinus; sqs, squamosal sinus. Colors indicate: green, turbinates; purple, mandibular canal and ramifications; orange, dentition; red, sinuses. Scale bar equals 10 cm.

to be somewhat shorter in Stock's (1925: Figure 60) illustration of *Paramylodon*.

The maxilloturbinates are also partially observable. They show the same anteroposterior elongation as the nasoturbinates, but their anatomical structure is more complex (**Figure 5A–D**). In fact, even if they are only partially preserved (broken in places and likely lacking the most delicate bony scrolls), they are clearly enrolled in a corkscrew fashion throughout most of their length (**Figure 5D**). The outermost scroll begins with a dorsolateral attachment to the inner wall of the nasal cavity, and then extends medially, curving ventrally as it approaches the nasal septum, then curving again medially, dorsally, and so on. Similarly scrolled maxilloturbinates are present in *Paramylodon harlani* (TJG, pers. observation). In ventral view, the maxilloturbinates of *Catonyx* appear thicker, forming a continuous surface, likely corresponding to the ventral concha (**Figures 5B,C**).

Cranial Sinuses

Cranial sinuses are well-developed in *Catonyx tarijensis* MNHN-Bol V 13364, extending for about two thirds of the entire skull length (**Figures 5A–C**). Pneumatization reaches its largest extent in the middle cranial area, where the sinuses mirror the external morphology of the cranium (**Figures 5A–C**). More posteriorly, at the level of the squamosal, parietal, and occipital bones, pneumatization is less dense or missing (**Figure 5**). This set of features is more similar to that of *Choloepus* (Boscaini et al., 2020) than that of other extinct giant sloths like *Glossotherium robustum* (Boscaini et al., 2020) and *Paramylodon harlani* (Stock, 1925), where the sinuses invade every bone all the way back to the occiput.

The frontal shows the highest level of pneumatization, with extensive sinuses extending from its anterior to posterior edges, in both dorsal and lateral views (**Figures 5A,C**). In lateral view, the extent of the sinuses reflects the anterior contact with both the lacrimal and the maxilla (**Figure 5C**). Frontal sinuses merge posteriorly with the orbitosphenoid and the alisphenoid sinuses. In fact, the latter bones are also largely pneumatized at the level of the common aperture for the optic foramen and sphenorbital fissure (**Figure 5C**), a common feature in extant and extinct sloths (Boscaini et al., 2020).

The squamosal of MNHN-Bol V 13364 is partially pneumatized, with large sinuses in its anteriormost portion, invading the tip of the zygomatic process (**Figures 5A–C**). However, the posterior half of the squamosal is not pneumatized

(**Figures 5A–C**), in contrast to *Glossotherium*, *Choloepus* and *Bradypus* (Boscaini et al., 2020). It should be noted that the squamosal pneumatization of the extant sloths is an epitympanic sinus continuous with the tympanic cavity ventrally, whereas that of *Catonyx* and *Glossotherium* is confined to the squamosal itself, as is typical for mylodontids (Gaudin, 1995). Parietal sinuses are observable in *Catonyx*, but only in proximity to the fronto-parietal suture (**Figures 5A–C**), as in *Choloepus* (Boscaini et al., 2020). In comparison to the frontal sinuses, the parietal sinuses are smaller in size, allowing observation of the underlying brain cavity in dorsal and lateral views (**Figures 5A–C**). In MNHN-Bol V 13364, sinuses at the level of the parietal represent the posteriormost extension of pneumatization, which is also lacking in most of the basicranium (**Figure 5**).

Ventrally, some sinuses were detected on the cranial base (**Figures 5B–E**). As already noted from the external aspect of MNHN-Bol V 13364, isolated sinuses are present in the pterygoid. They are placed in the middle of the descending lamina, but also posteriorly, at the posterior edge of the descending lamina (**Figures 5B–E**), as in *Glossotherium* and *Choloepus* (Boscaini et al., 2020). Moreover, some globose and individualized sinuses, similar to those of *Choloepus* (Boscaini et al., 2020), are visible in the basisphenoid, forming a "v-shaped" pneumatizatized area on the cranial base (**Figure 5B**). As in extant sloths (Boscaini et al., 2020), sinuses are lacking in the occipital (**Figure 5**).

Mandible and Dentition

The CT images of the mandible (**Figures 5F,G**) reveal the entire height of the lower teeth and the morphology of the mandibular canal. The left first, second, and fourth molariforms are pushed dorsally far out of their alveoli due to infilling sediment. The strongly hypselodont teeth once penetrated deeply in the mandible, reaching the mandibular canal.

The mandibular canal housed the mandibular division (V_3) of the trigeminal nerve, which exited the skull at the foramen ovale, entering the mandible through the internal aperture of the mandibular canal, located on the medial side of the coronoid process. As in all folivorans (Gaudin, 2004: char. 74), the mandibular canal also presents a posteroexternal opening on the lateral surface of the mandible.

The main branch of the mandibular canal is located ventrally in the dentary, extending medially to the lower dentition (**Figures 5F,G**). The most anterior portion of the mandibular canal diverges into several rami at the level of the mandibular spout, emerging from the numerous mental foramina (**Figures 5F,G**). The development of the mandibular canal and its rami reveal the many neurovascular terminations that occurred in this area.

Brain Endocast and Cranial Nerves

Brain endocast- The brain endocast of *Catonyx tarijensis* MNHN-Bol V 13364 (**Figure 6**) is generally similar to that of other mylodontid sloths and *Choloepus* (Gervais, 1869; Dechaseaux, 1958, 1962a,b, 1971; Boscaini et al., 2020), characterized by prominent olfactory bulbs, a globose telencephalon and mediolaterally expanded cerebellar hemispheres.

In dorsal view (**Figure 6A**), the olfactory bulbs of *Catonyx* are mediolaterally wide, as in *Glossotherium* and *Choloepus* (Boscaini et al., 2020). In MNHN-Bol V 13364, the olfactory bulbs are particularly protruded anteroposteriorly, and are connected to the telencephalon by two divergent olfactory peduncles (**Figure 6**). The olfactory bulbs are also dorsally directed in lateral view (**Figure 6C**) and appear elliptical in shape in anterior view (**Figure 6D**).

Compared to *Megatherium*, *Glossotherium*, and *Lestodon* (Dechaseaux, 1958, 1962a,b, 1971; Boscaini et al., 2020), the cerebrum of *Catonyx* is less domed in lateral view (**Figure 6C**). It is similar to *Choloepus* in this respect (Boscaini et al., 2020). In the same view, the telencephalon of *Catonyx* appears anteroposteriorly elongated, with prominent convolutions that are well-preserved on the left hemisphere. This convolution pattern consists of orbital, olfactory, suprasylvian, ectosylvian, and occipital gyri bordered by shallow furrows represented by the lateral, presylvian, suprasylvian, and pseudosylvian sulci, as well as by the rhinal and the transverse fissures (**Figure 6C**). The pyriform lobe is less developed than its homologue in *Glossotherium* (Boscaini et al., 2020), where it appears as a prominent bulge. In dorsal view (**Figure 6A**), the longitudinal fissure is barely visible on the anterior and posterior edges of the cerebrum, appreciable as slight surface inflections, whereas it is completely missing along its middle part. A weakly marked longitudinal fissure is also present in *Scelidotherium* (Gervais, 1869) and *Choloepus* (Boscaini et al., 2020) and differs from that in *Bradypus*, *Megatherium*, *Mylodon*, *Lestodon*, and *Glossotherium* (Gervais, 1869; Dechaseaux, 1958, 1962a,b, 1971; Boscaini et al., 2020), in which it is more marked and wider, particularly between the frontal lobes. Dorsally, both the frontal and temporal lobes are laterally expanded, crossed by wide gyri separated by slightly marked sulci. In dorsal view (**Figure 6A**), the lateral, suprasylvian, and occipital gyri, as well as the lateral and the entolateral sulci, are observable (**Figure 6A**). The general pattern of convolutions in *C. tarijensis* is comparable to that reported for *Glossotherium* and *Choloepus* (Dechaseaux, 1971; Boscaini et al., 2020).

More posteriorly, the cerebellum is mediolaterally expanded and separated from the cerebrum by a marked transverse fissure. As in *Lestodon*, *Mylodon*, *Scelidotherium*, *Megatherium*, *Choloepus* and *Glossotherium* (Gervais, 1869; Dechaseaux, 1958, 1962a,b, 1971; Boscaini et al., 2020), the cerebellar hemispheres are mediolaterally expanded and separated by a well-developed vermis (**Figure 6A**). In *Catonyx*, the strong development of the vermis and the marked transverse fissure are also particularly clear in lateral view (**Figure 6C**). As in *Glossotherium*, and in contrast to *Megatherium*, *Scelidotherium* and the extant sloths (Gervais, 1869; Dechaseaux, 1958, 1962a,b, 1971; Boscaini et al., 2020), the cerebellum appears wider mediolaterally in dorsal view than the posterior portion of the cerebrum (**Figure 6A**). However, when compared with *Glossotherium* (Boscaini et al., 2020), *Catonyx* shows a more anteroposteriorly compressed cerebellum (**Figure 6C**), similar to the condition observed in *Choloepus* (Boscaini et al., 2020).

Cranial nerves- Neither the ramifications of the olfactory nerves (I) nor the canals for the optic nerves (II) are preserved

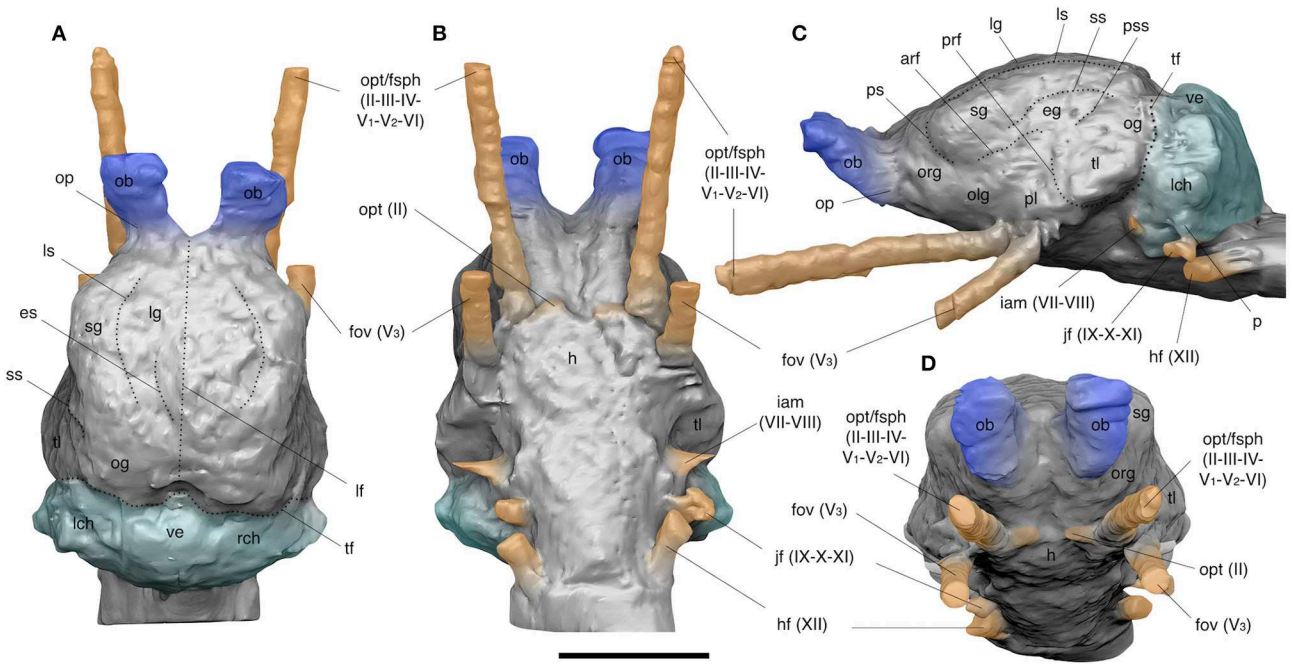

FIGURE 6 | Digital reconstructions of the brain cavity of *Catonyx tarijensis* MNHN-Bol V 13364 from the Pleistocene of Oruro (Bolivian Altiplano) in dorsal **(A)**, ventral **(B)**, lateral **(C)**, and anterior **(D)** views. arf, anterior rhinal fissure; eg, ectosylvian gyrus; es, entolateral sulcus; fov, foramen ovale groove; h, hypophysis; hf, hypoglossal foramen groove; iam, internal acoustic meatus; jf, jugular foramen groove; lch, left cerebellar hemisphere; lf, longitudinal fissure; lg, lateral gyrus; ls, lateral sulcus; ob, olfactory bulb; og, occipital gyrus; olg, olfactory gyrus; op, olfactory peduncle; opt, optic nerve; opt/fsph, common groove for the optic foramen and sphenorbital fissure; org, orbital gyrus; p, parafloccullus; pl, pyriform lobe; prf, posterior rhinal fissure; ps, presylvian sulcus; pss, pseudosylvian sulcus; rch, right cerebellar hemisphere; sg, suprasylvian gyrus; ss, suprasylvian sulcus; tf, transverse fissure; tl, temporal lobe; ve, vermis. Colors indicate: gray, cerebrum; blue, olfactory bulbs; turquoise, cerebellum; orange, neurovascular connections. Roman numeral designations indicate cranial nerves. Scale bar equals 5 cm.

in MNHN-Bol V 13364 (**Figure 6**). However, the impression of the optic chiasma itself is preserved, and it is likely that the optic nerve traveled some distance forward to merge with the sphenorbital fissure as in other mylodontids (Dechaseaux, 1971; Boscaini et al., 2020). In ventral view (**Figure 6B**), the common groove for the optic foramen and the sphenorbital fissure (accommodating cranial nerves II, III, IV, V_1, V_2, and VI), as well as that for the foramen ovale (housing V3, the mandibular branch of the trigeminal nerve), are the largest and most extended neurovascular canals in *Catonyx*. These openings are located at the level of the anteriormost portion of the brain (**Figures 6B–D**) and are more widely separated at their base than is the case in *Glossotherium*, in which the foramina converge at their origin (Boscaini et al., 2020). In lateral view, the sphenorbital fissure and the foramen ovale project forward strongly, forming an angle of about 30° to one another (**Figure 6C**). The internal acoustic meatus appears as a small bump located under the cerebellar hemispheres, close to the well-developed jugular and hypoglossal foramina (**Figure 6C**). The internal acoustic meatus is wider at its base and relatively larger than that of *Glossotherium* (Boscaini et al., 2020). In *Catonyx tarijensis* MNHN-Bol V 13364, the jugular and hypoglossal canals are similar in shape and close to each other (**Figures 6B–D**), whereas in *Glossotherium robustum* the hypoglossal is relatively larger and originates farther posteriorly (Boscaini et al., 2020). This is also reflected in the external cranial anatomy of *Catonyx* (see preceding section), and a similar condition was also observed in *Scelidotherium* (Gaudin, 2004; char. 187). In contrast, the hypoglossal foramen is larger than the jugular in *Mylodon* and *Glossotherium* (Patterson et al., 1992; Boscaini et al., 2018a).

DISCUSSION

The Pleistocene scelidotheriine sloth *Catonyx tarijensis* (Gervais and Ameghino, 1880) was first described on the basis of fossil remains recovered in the Tarija Valley (southern Bolivia). This locality is therefore the type locality of *C. tarijensis*, but it also represents the site that has provided the greatest number of skeletal remains for this species (Miño-Boilini, 2012). After the original description, many other remains referable to *C. tarijensis* were recovered in Argentina and Uruguay, extending its paleobiogeographic distribution to more southern latitudes in South America (McDonald and Perea, 2002; Corona et al., 2013; Miño-Boilini, 2016). The remains reported here represent the first record of this species from latitudes north of its type locality. They extend the geographic distribution of this taxon northward (**Figure 1**) and also expand the spectrum of paleoenvironments in which *C. tarijensis* could survive. Paleoenvironmental reconstructions of the Pleistocene of Tarija suggest the presence of open-county grasslands, with rivers and lakes surrounded by shrubs and scattered trees (Yoshida and Yamazaki, 1982; Coltorti et al., 2010; MacFadden et al., 2013).

The Bolivian Altiplano is distinguished by its higher altitude, but also its colder temperatures and dryer conditions relative to those recorded for the Tarija Valley. During the late Pleistocene, the Altiplano was characterized by periods of extreme dryness and shrinking bodies of water (Chepstow-Lusty et al., 2005; Coltorti et al., 2010). The recovery of *C. tarijensis* in the late Pleistocene of the Bolivian Altiplano suggests that this species could have been able to survive under a broad spectrum of paleoecological conditions.

The exceptional preservation of the skull of MNHN-Bol V 13364, together with its subadult ontogenetic stage, offer the opportunity for detailed observation of its external and internal anatomy, and to characterize some anatomical areas previously unknown for *Catonyx tarijensis*. The subadult age of MNHN-Bol V 13364 is indicated by the presence of many sutural contacts and the poorly developed temporal ridges and sagittal crest, as well as other features detected in the ear region, such as the narrow gap between the entotympanic and the basioccipital/basisphenoid tuber, the unusually deep stylohyal fossa, the presence of an open groove for the occipital artery on the paraoccipital process of the petrosal, and the reduced anteroventral process of the tegmen tympani (**Figures 2**, **3**). The presence of clear sutures in this skull has allowed us to observe the distinct outlines of many of the cranial bones for the first time, and have revealed at least one noteworthy, unusual feature, the small lateral exposure of the orbitosphenoid posterior to the aperture for the optic foramen/sphenorbital fissure (**Figure 2**). Another probable ontogeny-related feature is the occurrence of the lacrimal-nasal contact, which is absent in MNHN-Bol V 13364 (**Figure 2**), but figured as present in an adult *C. tarijensis* specimen by McDonald (1987). This feature was observed as variably present in *Scelidotherium leptocephalum* (Kraglievich, 1923) but its presence was later considered a synapomorphy of Scelidotheriinae by Gaudin (2004).

Other anatomical regions, such as the nasopharyngeal roof, the orbital foramina, and the hyoid apparatus are described in *Catonyx* for first time (**Figures 2**, **4**). Among these, the hyoid apparatus has been considered indicative of lingual anatomy and function, providing valuable information on the procurement and processing of dietary items in the oral cavity (Pérez et al., 2000, 2010). Although Pleistocene mylodontids were generally supposed to have had strong tongues, Pérez et al. (2010) suggested that *Scelidotherium* had significantly reduced lingual protrusion, when compared with the mylodontine *Glossotherium*. This was inferred mainly from the robust and barely mobile hyoid elements of *Scelidotherium*, which differ from the less rigidly articulated apparatus of *Glossotherium*. As a result, browsing species such as *S. leptocephalum* possessed long skulls and mandibular symphyses, and likely had strong prehensile lips but reduced lingual protrusion. In contrast, grazing species like *G. robustum* were characterized by shorter and broader skulls and mandibles, associated with reduced lips and increased lingual protrusion (Bargo et al., 2006; Bargo and Vizcaíno, 2008; Pérez et al., 2010). On the one hand, the hyoid apparatus of *Catonyx tarijensis* (**Figure 4**) bears a strong resemblance to that of *S. leptocephalum* (Pérez et al., 2010), further demonstrating that the morphology of the hyoid elements is phylogenetically informative (e.g., Gaudin, 2004; Casali and Perini, 2017; Zamorano, 2019). On the other hand, the strong similarity in the morphology of the hyoid apparatus among scelidotheriine sloths suggests similar feeding behaviors, characterized by limited lingual protrusion, with prehensile upper lips compensating for the less mobile tongue. Pérez et al. (2010) and Bargo et al. (2006) proposed that in narrow-muzzled sloths such as *Scelidotherium* and *Megatherium,* the upper lip was prehensile and used to select the plants. However, extinct sloths generally show a large mandibular canal, several foramina connected to the mandibular canal through multiple rami, including multiple mental foramina, as well as a wide posterior external opening of the mandibular canal, suggesting that the whole mandible was probably well-innervated and vascularized, especially in its anteriormost part (**Figure 5**). Accordingly, it is plausible that the lower lip also had greater mobility, contributing to better sensitivity and greater control of their grip on browse (**Figure 7**).

Strong bite movements concentrated in the mandible are also in accordance with the presence in MNHN-Bol V 13364 of two facets for the articulation of the mandible with cranial glenoid fossae (**Figure 2**). Moreover, the well-developed muscle scars in the ventral margin of the dentary are indicative of marked masticatory strength.

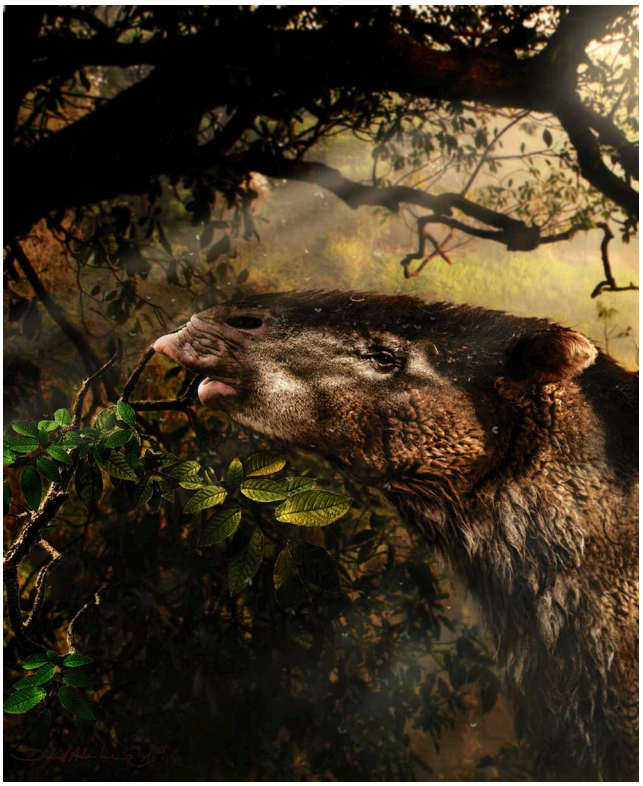

FIGURE 7 | Hypothetical life reconstruction of *Catonyx tarijensis* showing its inferred feeding behavior. The reconstruction is based on the skull MNHN-Bol V 13364 from the Pleistocene of Oruro (Bolivian Altiplano). Artwork by D. A. Iurino.

The digital model of the brain cavity of *Catonyx tarijensis* MNHN-Bol V 13364 (**Figure 6**) is extremely similar to that of *Glossotherium robustum* and *Choloepus hoffmanni* (Boscaini et al., 2020) and other giant extinct mylodontid sloths (Gervais, 1869; Dechaseaux, 1958, 1962a,b, 1971). In lateral view, only minor differences are observable between *C. tarijensis* and *G. robustum* in the shape of the olfactory bulbs, cerebral hemispheres, and cerebellum (Boscaini et al., 2020). Moreover, the pattern of sulci and gyri is extremely similar among extinct mylodontids sloths and the extant two-toed sloths (Boscaini et al., 2020). Although *Catonyx* and *Scelidotherium* show a weakly marked longitudinal fissure in comparison to other Mylodontidae, the general pattern of convolutions is similar to that in other members of the clade (Gervais, 1869; Dechaseaux, 1958, 1962a,b, 1971; Boscaini et al., 2018b, 2020). In general, the similar shape of the brain cavity and the shared pattern of convolutions among extinct mylodontid sloths and the living two-toed sloths, as well as the similar development of cranial sinuses in *Cholopeus* and the scelidotheriines (see below), is noteworthy. Indeed, recent molecular-based phylogenetic studies (i.e., Delsuc et al., 2019; Presslee et al., 2019) recovered the two-toed sloths as living representatives of Mylodontidae. Further CT-scanning data on other mylodontids and Antillean taxa is required to test this hypothesis, but the present study reveals the importance of accounting for novel morphological information from previously unexplored sources.

It should also be noted that there are also endocranial features which lack phylogenetic consistency among mylodontid sloths. Differences are evident in the pattern by which cranial nerves leave the brain cavity. As in *Glossotherium robustum*, but unlike extant sloths, *Catonyx tarijensis* possesses grooves for the optic foramen/sphenorbital fissure, the foramen ovale, and the hypoglossal foramen that are enlarged relative to other foramina transmitting cranial nerves (**Figure 6**; Boscaini et al., 2020). This suggests a greater development of the trigeminal and hypoglossal nerves, compared to other cranial nerves. However, in *C. tarijensis*, this relative difference in the size of cranial nerve grooves is not as marked as in *G. robustum*. This is particularly true for the groove for the hypoglossal nerve (XII), which is the only nerve leaving the skull from the hypoglossal foramen. In *Catonyx tarijensis* the hypoglossal foramen is roughly equivalent in size to the jugular foramen (**Figures 2**, **6**), whereas in *G. robustum* the hypoglossal foramen is larger (Boscaini et al., 2018a, 2020). The hypoglossal nerve, which innervates the glossal musculature, controls most of the intrinsic and extrinsic lingual musculature (Evans and de Lahunta, 2013). Together with evidence from the hyoid apparatus discussed above, this morphology can be viewed as further indirect evidence of more limited lingual protrusion of *C. tarijensis* in comparison to *G. robustum*.

Other differences between *Catonyx* and *Glossotherium* are noted in the morphology of their cranial sinuses. In general, cranial pneumatization is markedly reduced in the posteriormost portion of the skull of *C. tarijensis*, relative to that observed in *G. robustum* (Boscaini et al., 2020). As in *Choloepus* (Boscaini et al., 2020), the sinuses of *Catonyx* become smaller and more separate from one another at the frontoparietal suture, and are absent in the more posterior parts of the braincase (**Figure 5**). Preliminary observations suggest that this morphology is present in other Scelidotheriinae (Boscaini et al., 2018b), emphasizing the possible phylogenetic value of cranial pneumatization anatomy. In fact, for other large mammalian herbivores, the extent of cranial sinuses varies at the interspecific level according to both phylogeny and general body size (Farke, 2010). New body size estimations for mylodontid sloths (Boscaini et al., 2019b) predicted a larger body mass for *C. tarijensis* (∼1,640 kg) than *G. robustum* (∼1,480 kg), suggesting that among both xenarthrans and bovids (Farke, 2010), sinus organization could be driven primarily by phylogeny, and only secondarily related to general body mass.

However, the presence of functional or developmental constraints for explaining this alternative morphology cannot currently be refuted. Scelidotheriines have narrower heads than mylodontines and so may not have required as much pneumatization to reduce the weight of the head. However, it is also true that sinuses in sloths are more frequently present in the middle cranial region, extending posteriorly only in some cases (Boscaini et al., 2020), suggesting that this feature could be ontogeny-related. Thus, the question of the relative contributions of phylogeny and function to the pneumatic patterns observed in extinct sloths is clearly one that will require further study.

CONCLUSIONS

We report novel data on the external and internal cranial anatomy of the scelidotheriine sloth *Catonyx tarijensis*, further extending knowledge on the cranial morphology of South American extinct sloths. This discovery, from late Pleistocene deposits of the Department of Oruro (southwestern Bolivia), allowed us to extend the paleobiogeographic range of *C. tarijensis* to more northern latitudes, as well as to the high altitudes of the Bolivian Altiplano.

The specimen described in the present study, a particularly well-preserved skull with associated mandible and hyoid apparatus, corresponds to a subadult individual of *Catonyx tarijensis*. Combined information from the external and the internal anatomy, obtained through CT-scanning followed by digital modeling techniques, allowed us to analyze several anatomical regions that were unknown for this taxon.

Among these, the ear region, the nasopharyngeal area and the hyoid elements revealed several phylogenetically and functionally informative features. Digital models permitted observations of the brain cavity, neurovascular grooves and cranial sinuses, and comparisons of these features with other Pleistocene mylodontids.

The information presented in this report confirms previous hypotheses on inferred modes of food intake among extinct scelidotheriine sloths. According to the data now available, *C. tarijensis* was likely a browsing species, which tore vegetation mainly using its strong lips, rather than the tongue. This habit was probably common among Scelidotheriinae and contrasts with

that present in its sister clade, Mylodontinae, whose members were predominantly grazing species with smaller lips and more strongly protruding tongues.

The present study represents a further step in assembling broader morphological comparisons of digital endocranial models among extinct sloths, and emphasizes the importance of applying these new methodologies for understanding the evolution of this mammalian group.

DATA AVAILABILITY STATEMENT

All datasets generated for this study are included in the article/supplementary material.

AUTHOR CONTRIBUTIONS

AB, TG, DI, and FP conceived the paper. BM and RA collected and prepared the fossil specimen. DI and RS reconstructed the digital models. AB, TG, and DI wrote the paper with input from all authors. All authors contributed to the final version of the manuscript.

FUNDING

This research was funded by the National Geographic Society (projects NGS 9971-16 and EC-44712R-18). We are also particularly indebted to the MAECI (Ministry of Foreign Affairs and International Cooperation, Italy) for funding that greatly facilitated scientific collaboration between CONICET (Argentina) and Sapienza, Università di Roma (Italy), as well as funding from several sources at the University of Tennessee at Chattanooga.

ACKNOWLEDGMENTS

We are grateful to the Clínica Alemana Institute (La Paz, Bolivia) and the PaleoFactory Lab (Sapienza Università di Roma, Italy) for access to CT-scanning and digital modeling facilities. This research was made possible thanks to the cooperation agreement between the Bolivian institutions: GADOR (Gobernación Autónoma del Departamento de Oruro), GAM (Gobierno Autónomo Municipal) of Santiago de Andamarca, and MNHN-Bol. This paper greatly benefited from thoughtful comments and accurate revisions by three reviewers.

REFERENCES

Ameghino, F. (1891). Mamíferos y aves fósiles argentinas. Especies nuevas, adiciones y correcciones. *Rev. Argent. Hist. Nat.* 1, 240–259.

Ameghino, F. (1904). Nuevas especies de mamíferos cretáceos y terciarios de la república argentina. *An. Soc. Cient. Arg.* 58, 225–291.

Amson, E., Carrillo, J. D., and Jaramillo, C. (2016). Neogene sloth assemblages (Mammalia, *Pilosa*) of the cocinetas basin (La Guajira, Colombia): implications for the great American biotic interchange. *Palaeontology* 59, 563–582. doi: 10.1111/pala.12244

Bargo, M., Toledo, N., and Vizcaíno, S. F. (2006). Muzzle of South American Pleistocene ground sloths (*Xenarthra*, *Tardigrada*). *J. Morphol.* 267, 248–263. doi: 10.1002/jmor.10399

Bargo, M. S., and Vizcaíno, S. F. (2008). Paleobiology of pleistocene ground sloths (*Xenarthra*, *Tardigrada*): biomechanics, morphogeometry and ecomorphology applied to the masticatory apparatus. *Ameghiniana* 45, 175–196.

Boscaini, A., Iurino, D. A., Billet, G., Hautier, L., Sardella, R., Tirao, G., et al. (2018a). Phylogenetic and functional implications of the ear region anatomy of *Glossotherium robustum* (*Xenarthra*, *Mylodontidae*) from the Late Pleistocene of argentina. *Sci. Nat.* 105:28. doi: 10.1007/s00114-018-1548-y

Boscaini, A., Iurino, D. A., Cartelle, C., Strauss, A., De Iuliis, G., Sardella, R., et al. (2018b). "Digital endocranial reconstructions of the extinct scelidothere sloths (*Xenarthra*, *Mylodontidae*): emerging patterns in folivorans' evolution. IPC5," in *Abstract Book of the 5th International Palaeontological Congress* (Paris), 392.

Boscaini, A., Iurino, D. A., Sardella, R., Tirao, G., Gaudin, T. J., and Pujos, F. (2020). Digital cranial endocasts of the extinct sloth glossotherium robustum (*Xenarthra*, *Mylodontidae*) from the late pleistocene of argentina: description and comparison with the extant sloths. *J. Mammal. Evol.* 27, 55–71. doi: 10.1007/s10914-018-9441-1

Boscaini, A., Pujos, F., and Gaudin, T. J. (2019a). A reappraisal of the phylogeny of *Mylodontidae* (*Mammalia*, *Xenarthra*) and the divergence of mylodontine and lestodontine sloths. *Zool. Scr.* 48, 691–710. doi: 10.1111/zsc.12376

Boscaini, A., Toledo, N., Soto, I. M., Gaudin, T. J., and Pujos, F. (2019b). "Filogenia y evolución del tamaño corporal en perezosos milodóntidos (*Mammalia, Xenarthra, Folivora*)," in *RCAPA 2019. Abstract Book of the "Reunión de Comunicaciones de la Asociación Paleontológica Argentina"* (La Plata), 91.

Brambilla, L., and Ibarra, D. A. (2018). The occipital region of late pleistocene *Mylodontidae* of argentina. *Bol. Inst. Fis. Geol.* 88, 1–9.

Cartelle, C., De Iuliis, G., Boscaini, A., and Pujos, F. (2019). Anatomy, possible sexual dimorphism, and phylogenetic affinities of a new mylodontine sloth from the late Pleistocene of intertropical Brazil. *J. Syst. Palaeontol.* 17, 1957–1988. doi: 10.1080/14772019.2019.1574406

Cartelle, C., De Iuliis, G., and Lopes Ferreira, R. (2009). Systematic revision of tropical Brazilian scelidotheriine sloths (*Xenarthra*, *Mylodontoidea*). *J. Vertebr. Paleontol.* 29, 555–566. doi: 10.1671/039.029.0231

Casali, D. M., and Perini, F. A. (2017). The evolution of hyoid apparatus in *Xenarthra* (*Mammalia*: *Eutheria*). *Hist. Biol.* 29, 777–788. doi: 10.1080/08912963.2016.1241248

Chepstow-Lusty, A., Bush, M. B., Frogley, M. R., Baker, P. A., Fritz, S. C., and Aronson, J. (2005). Vegetation and climate change on the bolivian Altiplano between 108,000 and 18,000 years ago. *Quaternary Res.* 63, 90–98. doi: 10.1016/j.yqres.2004.09.008

Coltorti, M., Abbazzi, L., Ferretti, M. P., Iacumin, P., Ríos, F. P., Pellegrini, M., et al. (2007). Last glacial mammals in South America: a new scenario from the Tarija Basin (Bolivia). *Naturwissenschaften* 94, 288–299. doi: 10.1007/s00114-006-0196-9

Coltorti, M., Pieruccini, P., and Paredes, F. R. (2010). Late pleistocene stratigraphy, sedimentology and paleoenvironmental evolution of the Tarija-Padcaya basin (Bolivian Andes). *P. Geologist. Assoc.* 121, 162–179. doi: 10.1016/j.pgeola.2010.04.002

Cope, E. D. (1889). The edentata of North America. *Am. Nat.* 23, 657–664. doi: 10.1086/274985

Corona, A., Perea, D., and McDonald, H. G. (2013). *Catonyx cuvieri* (*Xenarthra*, *Mylodontidae*, *Scelidotheriinae*) from the late pleistocene of Uruguay, with comments regarding the systematics of the subfamily. *J. Vertebr. Paleontol.* 33, 1214–1225. doi: 10.1080/02724634.2013.764311

Dechaseaux, C. (1958). "Encéphales de xénarthres fossiles," in *Traité de Paléontologie*, ed J. Piveteau (Paris: Masson and Cie), 637–640.

Dechaseaux, C. (1962a). Encéfalos de notongulados y de desdentados xenarthros fósiles. *Ameghiniana* 2, 193–209.

Dechaseaux, C. (1962b). Singularités de l'encéphale de *Lestodon*, mammifère édenté géant du Pléistocène d'Amérique du Sud. *C. R. Acad. Sci.* 254, 1470–1471.

Dechaseaux, C. (1971). *Oreomylodon wegneri*, édenté gravigrade du Pléistocène de l'Équateur - Crâne et moulage endocrânien. *Ann. Paléontol.* 57, 243–285.

Delsuc, F., Catzeflis, F. M., Stanhope, M. J., and Douzery, E. J. (2001). The evolution of armadillos, anteaters and sloths depicted by nuclear and mitochondrial phylogenies: implications for the status of the enigmatic fossil *Eurotamandua*. *Proc. R. Soc. B* 268, 1605–1615. doi: 10.1098/rspb.2001.1702

Delsuc, F., Kuch, M., Gibb, G. C., Karpinski, E., Hackenberger, D., Szpak, P., et al. (2019). Ancient mitogenomes reveal the evolutionary history and biogeography of sloths. *Curr. Biol.* 29, 2031–2042.e6. doi: 10.1016/j.cub.2019.05.043

Evans, H. E., and de Lahunta, A. (2013). *Miller's Anatomy of the Dog*. St. Louis: Elsevier.

Farke, A. A. (2010). Evolution and functional morphology of the frontal sinuses in *Bovidae* (*Mammalia*: Artiodactyla), and implications for the evolution of cranial pneumaticity. *Zool. J. Linn. Soc.* 159, 988–1014. doi: 10.1111/j.1096-3642.2009.00586.x

Flower, W. (1883). On the arrangement of the orders and families of existing *Mammalia*. *Proc. Zool. Soc. Lond.* 1883, 178–186.

Gaudin, T. J. (1995). The ear region of edentates and the phylogeny of the *Tardigrada* (*Mammalia*, *Xenarthra*). *J. Vertebr. Paleontol.* 15, 672–705. doi: 10.1080/02724634.1995.10011255

Gaudin, T. J. (2004). Phylogenetic relationships among sloths (*Mammalia, Xenarthra, Tardigrada*): the craniodental evidence. *Zool. J. Linn. Soc.* 140, 255–305. doi: 10.1111/j.1096-3642.2003.00100.x

Gaudin, T. J. (2011). On the osteology of the auditory region and orbital wall in the extinct West Indian sloth genus *Neocnus* Arredondo, 1961 (*Placentalia*, *Xenarthra*, *Megalonychidae*). *Ann. Carnegie Mus.* 80, 5–28. doi: 10.2992/007.080.0102

Gaudin, T. J., and Croft, D. A. (2015). Paleogene *Xenarthra* and the evolution of South American mammals. *J. Mammal.* 96, 622–634. doi: 10.1093/jmammal/gyv073

Gervais, H., and Ameghino, F. (1880). *Los mamíferos fósiles de la América del Sud*. Paris: F. Savy and Buenos Aires: Hermanos Igon.

Gervais, P. (1869). Mémoire sur les formes cérébrales propres aux édentés vivants et fossiles. *Nouv. Arch. Mus. Hist. Nat. Paris* 5, 1–56.

Gill, T. (1872). Arrangement of the families of mammals, with analytical tables. *Smithson. Misc. Collect.* 11, 1–98.

Hirschfeld, S. E. (1985). Ground sloths form the friasian la venta fauna, with additions to the pre-friasian coyaima fauna of Colombia, South America. *Univ. Calif. Publ. Geol. Sci.* 128, 1–91.

Kraglievich, L. (1923). Descripción comparada de los cráneos de "*Scelidodon Rothi*" Amegh. y "*Scelidotherium Parodii*" n. sp. procedentes del horizonte "Chapadmalense." *Anales Mus. Nac. Hist. Nat. Buenos Aires* 33, 57–103.

MacFadden, B. J., Zeitler, P. K., Anaya, F., and Cottle, J. M. (2013). Middle pleistocene age of the fossiliferous sedimentary sequence from Tarija, Bolivia. *Quarter. Res.* 79, 268–273. doi: 10.1016/j.yqres.2012.12.009

McDonald, H. G. (1987). A systematic review of the plio-pleistocene scelidotherine ground sloth (*Mammalia: Xenarthra: Mylodontidae*) (Ph.D. Dissertation). University of Toronto, Toronto, ON, Canada.

McDonald, H. G. (1997). "Xenarthrans: pilosans," in *Vertebrate Paleontology in the Neotropics. The Miocene Fauna of La Venta, Colombia*, eds. R. F. Kay, R. H. Madden, R. L. Cifelli, and J. J. Flynn (Washington and London: Smithsonian Institution Press), 233–245.

McDonald, H. G. (2005). Paleoecology of extinct xenarthrans and the great biotic interchange. *Bull. Fla. Mus. Nat. Hist.* 45, 319–340.

McDonald, H. G., and De Iuliis, G. (2008). "Fossil history of sloths," in *The Biology of the Xenarthra*, eds *S. F. Vizcaíno and W. J. Loughry* (Gainesville, FL: University Press of Florida), 39–55.

McDonald, H. G., and Pelikan, S. (2006). Mammoths and mylodonts: exotic species from two different continents in North American pleistocene faunas. *Quatern. Int.* 142–143, 229–241. doi: 10.1016/j.quaint.2005.03.020

McDonald, H. G., and Perea, D. (2002). The large scelidothere *Catonyx tarijensis* (*Xenarthra, Mylodontidae*) from the Pleistocene of Uruguay. *J. Vertebr. Paleontol.* 22, 677–683. doi: 10.1671/0272-4634(2002)022<0677:TLSCTX>2.0.CO;2

McNab, B. K. (1985). "Energetics, population biology, and distribution of Xenarthrans, living and extinct," in *The Evolution and Ecology of Armadillos, Sloths and Vermilinguas,* ed G. G. Montgomery (Washington, DC: Smithsonian Institution Press), 219–232.

Miño-Boilini, Á. R. (2012). *Sistemática y Evolución de los Scelidotheriinae (Xenarthra, Mylodontidae) Cuaternarios de la Argentina. Importancia Bioestratigráfica, Paleobiogeográfica y Paleoambiental* (Ph.D. Dissertation), Universidad de La Plata, La Plata, Argentina.

Miño-Boilini, Á. R. (2016). Additions to the knowledge of the ground sloth *Catonyx tarijensis* (*Xenarthra*, *Pilosa*) in the pleistocene of argentina. *Paläontol. Z.* 90, 173–183. doi: 10.1007/s12542-015-0280-6

Miño-Boilini, Á. R., De Los Reyes, M., Zurita, A. E., Arrouy, M. J., and Poiré, D. G. (2019). Pliocene scelidotheriinae (*Xenarthra, Tardigrada*) from the pampean region of argentina: morphology, chronology, and comments on the diversity of the subfamily. *C. R. Palevol,* 18, 325–334. doi: 10.1016/j.crpv.2019.01.005

Naples, V. L. (1986). The morphology and function of the hyoid region in the tree sloths, *Bradypus* and *Choloepus*. *J. Mammal.* 67, 712–724. doi: 10.2307/1381132

Nowak, R. M. (1999). *Walker's Mammals of the World*. Baltimore; London: The John Hopkins University Press.

Owen, R. (1839). "Fossil Mammalia," in *The Zoology of the Voyage of H.M.S. Beagle, Under the Command of Captain Fitzroy, During the Years 1832 to 1836*, ed C. Darwin (London: Smith, Elder & Co.), 41–80.

Owen, R. (1857). On the scelidothere (*Scelidotherium leptocephalum*, Owen). *Philos. Trans. R. Soc. Lond.* 147, 101–110. doi: 10.1098/rstl.1857.0008

Patterson, B., Turnbull, W. D., Segall, W., and Gaudin, T. J. (1992). The ear region in xenarthrans (=Edentata: *Mammalia*). Part II. Pilosa (sloths, anteaters), palaeanodonts, and a miscellany. *Fieldiana Geol.* 24, 1–78. doi: 10.5962/bhl.title.3466

Pérez, L. M., Scillato-Yané, G. J., and Vizcaíno, C. F. (2000). Estudio morfofuncional del aparato hioideo de *Glyptodon* cf. *clavipes* Owen (*Cingulata*: *Glyptodontidae*). *Ameghiniana* 37, 293–300.

Pérez, L. M., Toledo, N., De Iuliis, G., Bargo, M. S., and Vizcaíno, S. F. (2010). Morphology and function of the hyoid apparatus of fossil xenarthrans (*Mammalia*). *J. Morphol.* 271, 1119–1133. doi: 10.1002/jmor.10859

Placzek, C., Quade, J., and Patchett, P. J. (2006). Geochronology and stratigraphy of late pleistocene lake cycles on the southern bolivian altiplano: implications for causes of tropical climate change. *GSA Bull.* 118, 515–532. doi: 10.1130/B25770.1

Presslee, S., Slater, G. J., Pujos, F., Forasiepi, A. M., Fischer, R., Molloy, K., et al. (2019). Palaeoproteomics resolves sloth relationships. *Nat. Ecol. Evol.* 3, 1121–1130. doi: 10.1038/s41559-019-0909-z

Pujos, F. (2000). *Scelidodon chiliensis* (*Xenarthra, Mammalia*) du Pléistocène terminal de "Pampa de los Fósiles". *Quaternaire* 11, 197–206. doi: 10.3406/quate.2000.1669

Pujos, F., Gaudin, T. J., De Iuliis, G., and Cartelle, C. (2012). Recent advances on variability, morpho-functional adaptations, dental terminology, and evolution of sloths. *J. Mammal. Evol.* 19, 159–169. doi: 10.1007/s10914-012-9189-y

Robertson, J. S. (1976). Latest Pliocene mammals from Haile XV A, Alachua County, Florida. *Bull. Fla. Mus. Nat. Hist.* 20, 111–186.

Scillato-Yané, G. J., and Carlini, A. A. (1998). Nuevos xenarthra del friasense (Mioceno medio) de Argentina. *Stvd. Geol. Salmant.* 34, 43–67.

Steadman, D. W., Martin, P. S., MacPhee, R. D. E., Jull, A. J. T., McDonald, H. G., Woods, C. A., et al. (2005). Asynchronous extinction of late quaternary sloths on continents and islands. *Proc. Natl. Acad. Sci. U.S.A.* 102, 11763–11768. doi: 10.1073/pnas.0502777102

Stock, C. (1925). Cenozoic gravigrade edentates of Western North America with special reference to the pleistocene megalonychinae and mylodontidae of Rancho La Brea. *Carnegie Inst. Wash. Publ.* 331, 1–206.

Tambusso, P. S., McDonald, H. G., and Fariña, R. A. (2015). Description of the stylohyal bone of a giant sloth (*Lestodon armatus*). *Palaeontol. Electron.* 18, 1–10. doi: 10.26879/506

Vizcaíno, S. F., Zárate, M., Bargo, M. S., and Dondas, A. (2001). Pleistocene burrows in the Mar del Plata area (Argentina) and their probable builders. *Acta Palaeontol. Pol.* 46, 289–301.

Webb, S. D. (1989). "Osteology and relationships of thinobadistes segnis, the first mylodont sloth in North America," in *Advances in Neotropical Mammalogy*, eds K. H. Redford and J.F. Eisenberg (Gainesville, FL: Sandhill Crane Press), 469–532.

Yoshida, A., and Yamazaki, E. (1982). "Micro-fossils," in *Tarija mammal-bearing formation in Bolivia*, ed F. *Takai* (Tokyo: Research Institute of Evolutionary Biology), 57–62.

Zamorano, M. (2019). Análisis filogenético de xenartros (*Mammalia*) basados en elementos óseos del aparato hioides: aspectos sobre la monofilia de gliptodóntidos. *Rev. Bras. Paleontolog.* 22, 53–66. doi: 10.4072/rbp.2019.1.05

Conflict of Interest: The authors declare that the research was conducted in the absence of any commercial or financial relationships that could be construed as a potential conflict of interest.

The reviewer GD, declared a past collaboration with the authors to the handling editor.